2 Near-IR kinetic spectroscopy (IR-KS) of the HO_2 and $C_2H_5O_2$ self and cross Reactions

2.1 Introduction

The chemistry of alkyl peroxy radicals (RO_2), introduced in Chapter 1, is central to the oxidation of volatile organic compounds (VOCs) in the atmosphere. In the troposphere RO_2 react primarily under two different regimes: high NO_x and low NO_x. Under the high NO_x conditions of urban air RO_2 chemistry contributes to regional air pollution problems by producing O_3. In the unpolluted troposphere (NO_x < ~20 pptv) the primary loss pathways for RO_2 radicals are self reaction and cross reaction with HO_2. These reactions lead to the production of organic hydroperoxides (ROOH), which are a temporary reservoir for HO_x. The net effect is to slow down or eliminate the production of O_3 from RO_2 chemistry.[1,2]

Ethane is one of the most abundant non methane hydrocarbons with a globally averaged annual concentration of ~ 1 ppb.[3] The ethyl peroxy radical ($C_2H_5O_2$) is formed in the atmosphere predominantly from the oxidation of ethane.

$$C_2H_6 + OH \xrightarrow{O_2} C_2H_5O_2 \qquad (2.1)$$

In the remote troposphere the dominant loss process will be reaction with HO_2,

$$C_2H_5O_2 + HO_2 \longrightarrow C_2H_5OOH + O_2 \qquad (2.2)$$

which leads to the formation of ethyl hydroperoxide (C_2H_5OOH). The concentrations of both $C_2H_5O_2$ and HO_2 also depend on their self reactions.

$$C_2H_5O_2 + C_2H_5O_2 \longrightarrow \text{products} \qquad (2.3)$$

$$\longrightarrow C_2H_5O + C_2H_5O + O_2 \qquad (2.3a)$$

$$\longrightarrow C_2H_5OH + CH_3CHO + O_2 \qquad (2.3b)$$

$$\longrightarrow C_2H_5OOC_2H_5 + O_2 \qquad (2.3c)$$

$$C_2H_5O + O_2 \longrightarrow HO_2 + CH_3CHO \qquad (2.4)$$

$$HO_2 + HO_2 \xrightarrow{M} HOOH + O_2 \qquad (2.5)$$

Reaction (2.4) is a critical link because it leads to the generation of secondary HO_2. This recycles radicals in the atmosphere, and complicates laboratory kinetics experiments. The competition between the self, (2.3) and (2.5), and cross (2.2) reactions means that a pseudo-first-order kinetics experiment is not possible when trying to measure the rate coefficient for reaction (2.2), k_2, and that no analytic solution to the kinetics equations for the reaction exist.

There have been a number of studies of the kinetics[4-9] and products[9-12] of reaction (2.2). All of the kinetics studies with the exception of Cattell et al.[5] and Raventos-Duran et al.[9] used UV absorption alone to monitor peroxy radicals. One problem with UV absorption is that all RO_2 radicals have overlapping broad absorption features arising from a $\pi \rightarrow \pi^*$ transition on the terminal oxygen atom. This overlap of the $C_2H_5O_2$ and HO_2 absorption bands increases the uncertainty of the derived rate coefficient(s). A second problem with UV absorption is that it is not a particularly sensitive method unless long path lengths are used (several meters). This limits the range of initial reaction ratios, $[HO_2]_0 / [C_2H_5O_2]_0$, that can be used to check for consistency in the kinetics model. A different complication that affected several of the previous temperature-dependent measurements is the use of CH_3OH as a precursor for HO_2.[6,7] It has been demonstrated in this lab and others that CH_3OH acts as a chaperone, leading to larger apparent HO_2 self reaction rate constants at low temperature.[12,13] The large variation in the reported range

of $\frac{E_A}{R}$ (650-1250 K^{-1}), is evidence of the difficulties encountered by previous temperature-dependent studies. The product studies on reaction (2.2) were done with FTIR and chemical ionization mass spectrometry (CIMS), and they showed that C_2H_5OOH is the major product.

The self reaction kinetics of $C_2H_5O_2$ were also measured by a number of groups,[5,7,10,11,14-19] and separate product studies were completed to determine the branching ratios of the different channels.[11,14,20-22] The difficulty with studying reaction (2.3) is that the alkoxy products in (2.3a) can go on to produce secondary HO_2 by reaction (2.4). This secondary HO_2 will enhance the apparent rate of reaction (2.3). It is possible to determine the actual rate constant for reaction (2.3) from the observed if the branching fraction to the alkoxy channel α is known.[23]

$$k_3 = \frac{k_{3obs}}{1+\alpha} \quad \text{(i)}$$

$$\alpha = \frac{k_{3a}}{k_3} \quad \text{(ii)}$$

All of the previous kinetics experiments used UV absorption to measure k_{3obs} and used α from end product studies to determine k_3. The end product studies on reaction (2.3) are in fair agreement, but there has been no measurement of α below room temperature. There also has been no measurement of α by a direct observation of the nascent products.

This study aimed to overcome some of the difficulties in previous work by using two probes in different wavelength regions to characterize the above reactions. A near-infrared (NIR) probe measured HO_2 and an ultraviolet (UV) probe measured $C_2H_5O_2$. Experiments were done either focusing on (2.2) or (2.3). The rate coefficient k_2 was

measured during experiments on (2.2). In the experiments focusing on reaction (2.3) UV detection of $C_2H_5O_2$ allowed for the determination of k_{3obs} similar to previous studies. In addition, the NIR measured the time profile of secondary HO_2 from reactions (2.3) and (2.4), allowing for real time determination of α and k_3 for the first time. The measurements made of each reaction were then used together to develop a self consistent description of the self and cross reactions of $C_2H_5O_2$ and HO_2.

2.2 Experimental

2.2.1 Summary

The experimental apparatus is discussed in Chapter 5, and has been given in full detail previously.[24] Briefly, the IRKS apparatus consisted of a flash photolysis flow cell coupled with two optical probes for time-resolved HO_2 and $C_2H_5O_2$ detection. An excimer laser created a column of radicals down the length of the ~ 2 m flow cell. $C_2H_5O_2$ was detected by UV absorption spectroscopy. The UV light from a deuterium lamp was coupled into the cell along the same path as the excimer but in a counter-propagating direction. A monochromator was used to select the desired wavelength from the light exiting the cell. HO_2 was detected at the overtone of its OH stretching vibration using NIR wavelength modulation (WM) spectroscopy. The NIR light was also coupled lengthwise but was slightly off axis compared to the excimer and deuterium lamp. The NIR beam begins above and ends below the deuterium and excimer beams, but makes 30 passes crossing through the photolysis region in a Herriott cell setup. Data acquisition was gated to the firing of the excimer, and data for both optical probes were recorded simultaneously. The data from both probes were then fit simultaneously to determine the desired kinetics parameters.

2.2.2 Apparatus and Detection Probes

The radical chemistry took place in a 175 cm long, 5 cm diameter reaction cell. The intersection of the reactant gases with the excimer laser defined the photolysis volume, 2 cm x 1 cm x 138 (159) cm. The gas flows were adjusted so that the residence time in the flow cell (typically 10–15 s) matched the interval between photolysis laser pulses. Photolysis of Cl_2 by a XeCl excimer laser (308 nm, 110 ± 15 mJ/pulse) led to the formation of HO_2 and $C_2H_5O_2$ by the reaction sequence,

$$\mathrm{Cl_2} + h\nu(308\ \mathrm{nm}) \longrightarrow 2\mathrm{Cl} \tag{2.6}$$

$$\mathrm{Cl} + \mathrm{CH_3OH} \longrightarrow \mathrm{CH_2OH} + \mathrm{HCl} \tag{2.7}$$

$$\mathrm{Cl} + \mathrm{C_2H_6} \longrightarrow \mathrm{C_2H_5} + \mathrm{HCl} \tag{2.8}$$

$$\mathrm{CH_2OH} + \mathrm{O_2} \longrightarrow \mathrm{HO_2} + \mathrm{HCHO} \tag{2.9}$$

$$\mathrm{C_2H_5} + \mathrm{O_2} \xrightarrow{\mathrm{M}} \mathrm{C_2H_5O_2} \tag{2.10}$$

For the experiments on the $C_2H_5O_2$ self reaction no CH_3OH was used, but there is a small source of HO_2 from the reaction that forms $C_2H_5O_2$.

$$\mathrm{C_2H_5} + \mathrm{O_2} \longrightarrow \mathrm{HO_2} + \mathrm{C_2H_4} \tag{2.11}$$

The HO_2 concentration resulting from reaction (2.11) is about 1% of the initial $C_2H_5O_2$. This value is in good agreement with previous work by Kaiser et al., but is slightly higher than new measurements by Clifford et al.[25-27]

The temperature in the cell was held to within ± 1 K of the stated temperatures. Methanol cooled by liquid nitrogen circulated through a jacket around the cell to obtain temperatures below 298 K. Calibrated flows of reagent gases were cooled and mixed in a 1 m long tube before flowing into the middle of the reaction cell. The temperature

inside the cell was measured with a type T thermocouple (Omega). A purge flow was used to protect the NIR Herriott mirrors from corrosion and contain the main flow to the temperature-controlled region. The mixing of the purge flow and reactant gases occurred throughout 10 cm on either side of the cell leading to a path length of 148 ± 10 cm. A complete discussion of the purge and reactant gas mixing is given in Chapter 5.

Typical reagent gas concentrations were, in units of molecules cm^{-3}: Cl_2 = (0.3-1.5) × 10^{16}, He = (3-15) × 10^{16}, CH_3OH = (0–2.5) × 10^{15}, C_2H_6 = (0.5–30) × 10^{15}, O_2 = (5-20) × 10^{17}, N_2 = (0-1) × 10^{18}. The CH_3OH was carried into the cell by N_2 after it passed through the liquid CH_3OH (J.T. Baker, PHOTOREX® Reagent) in a bubbler held at 273 K. The experiments on the cross reaction (2.2) were performed in O_2. The $C_2H_5O_2$ self reaction (2.3) measurements were primarily in O_2 as well, but used N_2 as a buffer when investigating the effect of varying O_2 concentrations on α. All gas flows were monitored with mass flow meters (Hastings HFM-200 series) and controlled with needle valves. Sufficient concentrations of C_2H_6 and/or CH_3OH were always used to insure stochiometric conversion of Cl to $C_2H_5O_2$, HO_2 or both. In the experiments on (2.2) flows were adjusted to investigate the kinetics over a wide range of initial radical concentrations, i.e., different values of the initial radical ratio: $[HO_2]_0 / [C_2H_5O_2]_0$. This ratio typically ranged from 0.1–4 while the total concentration of radicals remained constant at ~ 1 x 10^{14} molecules cm^{-3}. For experiments on (2.3) the total radical concentration was varied, typically from 3.0 x 10^{13}– 1.5 x 10^{14} molecules cm^{-3}. At least six measurements were made spaced throughout the range of the initial radical ratio, or total radical concentration, at every temperature and pressure for (2.2) and (2.3), respectively. The pressures in the cell and the CH_3OH bubbler were monitored by

capacitance manometers (MKS-220CA 1000 Torr), and were constant within ± 2 Torr of the stated pressures. Flow meters were calibrated by measuring the time required to flow through a calibrated volume over a range of flows suitable to each meter. The capacitance manometers were calibrated in reference to other factory calibrated capacitance manometers.

Two optical probes were used to monitor the radical chemistry. The UV light source was a 150 W deuterium lamp (Hamammatsu L1314). The beam made a single pass through the cell counter-propagating with the excimer photolysis beam. Baffles on either end of the reaction cell ensured that only light that had sampled the photolysis region entered the monochromator slit. The monochromator was set to 250.0 nm for detection of $C_2H_5O_2$. The minimum detectable absorbance for $C_2H_5O_2$ was ~ 2 x 10^{-5} Hz $^{-1/2}$ (~ 6 x 10^{12} molecules cm^{-3}). The monochromator was calibrated by looking at the atomic emission lines from a Hg pen lamp. The NIR probe source was a 3 mW distributed-feedback (DFB) continuous-wave tunable diode laser manufactured in the JPL Microdevices Laboratory. The laser was tuned for HO_2 at the $^qQ_2$ band head (6638.2 cm^{-1}) of the first overtone of the OH stretch.[28] The NIR beam made 30 passes through the reaction cell using a Herriott cell setup with an estimated effective path length of 2700 cm. The laser was frequency modulated at 6.8 MHz by varying the drive current with an external RF generator. The signal from the InGaAs photodiode detector (New Focus 1811) was demodulated at 13.6 MHz (2f detection) and subsequently amplified by a factor of 100. The minimum detectable absorbance for HO_2 was ~ 2 x 10^{-7} Hz $^{-1/2}$ (~ 1 x 10^{11} molecules cm^{-3}).

The detector signals for both optical probes were recorded simultaneously. The data acquisition was controlled by a Visual BASIC program. For reaction (2.2) the decay measurements typically began 1 ms before the excimer fired to establish a baseline for the signal, and continued for 20 ms at a sampling rate of 200 kS/s. For reaction (2.3) the baseline was recorded for 10 ms before the excimer pulse and continued for 200 ms at a sampling rate of 20 kS/s to capture the slower decay. Both signals were low pass filtered at 100 kHz and 10 kHz, respectively (SRS-SR560). The data was digitized using a two channel 16 bit per channel A/D card with a maximum sampling rate of 2.5 MS/s (Gage-CompuScope 1602). Decay traces for the UV and the IR probes were obtained by averaging the signals over 50 excimer shots.

2.2.3 Calibration of the NIR Probe

The NIR probe was calibrated daily to measure HO_2 because WM spectroscopy measures relative not absolute changes in concentration. The NIR probe was calibrated with the UV absorption probe by measuring the kinetics of the HO_2 self-reaction (2.5). The two probe beams measure the same physical processes, albeit with different geometrical overlap, but should yield the same bimolecular kinetics at short time scales (~ 20 ms). At the beginning of each day data for reaction (2.5) were taken while only HO_2 radicals were present. The UV monochromator was set to 220.0 nm to monitor HO_2 at the same as it was monitored by the NIR. The time decays of both probes were fit simultaneously with the kinetics modeling program FACSIMILE.[29] The fits checked for consistency between the probes, and determined that day's calibration factor for the NIR. The rate coefficient of the HO_2 self reaction k_5 used in the kinetic modeling of (2.2) and (2.3) was taken from these daily measurements as it was determined along with the value

of the calibration factor for the NIR. This calibration factor was very sensitive to optical alignment, but in general was consistent from day to day within ± 15%. The UV detection wavelength was then optimized for $C_2H_5O_2$ detection to allow for the simultaneous independent detection of both radicals.

2.2.4 Diffusion

Diffusion was taken into account when modeling the data and comparing the two probes. For reactions that were complete in < 20 ms diffusion had a minimal effect, but all data was treated the same way. Different volumes of the reaction cell were sampled by the UV and NIR probes, and this led to different observed behavior from diffusion. UV modeling included an explicit loss term, but The NIR had offsetting effects that were not factored into the kinetics model. The UV was co-aligned with the excimer laser down the middle of the flow cell. The radicals created down the middle of the cell diffused radially out of the UV beam given sufficient time. This type of diffusion was approximated as a unimolecular loss term in the kinetic fits. By varying the initial concentration of total radicals and determining the observed bimolecular rate constant, the contribution of diffusion to the observed rate constant was determined in the manner of Thiebaud et al.[30] The NIR was complicated by the geometry of the Herriott cell. The NIR beam passed in and out of the photolysis region because of its off axis alignment with respect to the radicals. Diffusion allowed parts of the beam originally outside the photolysis region to interact with radicals and extend the path length. However the concentration profile along that path length was not uniform. The different concentrations underwent reaction at different rates. At longer times, as more and more of the beam passed through smaller concentrations of the radical, the bimolecular reaction rate appeared to have slowed

down. This led to a small systematic residual in the IR signal. This effect on the overall error analysis will be discussed in the results and analysis section.

2.3 Results and analysis

2.3.1 Overview

Reactions (2.2) and (2.3) were the primary focus of this work. In order to achieve the greatest sensitivity to k_2 and k_3 one type of experiment was performed in which both HO_2 and $C_2H_5O_2$ were created deliberately, and another type where only $C_2H_5O_2$ was created deliberately. Both types of experiment were done using simultaneous NIR and UV probes of HO_2 and $C_2H_5O_2$, respectively. Perfect isolation of each reaction is not possible because they are connected by secondary chemistry, but one reaction or the other became the focus with the different experimental conditions. The rate coefficients k_2 and k_3 and the branching fraction α were measured in a self consistent manner. Correlation among the parameters was explored and accounted for throughout the data analysis.

2.3.2 Methods and Error Analysis

All three of the major kinetics parameters determined in this study – k_2, k_3, and α – could not be well determined at the same time. Unphysical values for the parameters were returned when all three were varied at once. Therefore it was necessary to follow an iterative procedure for fitting the data. First the NIR was calibrated with data from (2.5) as described in the experimental section on NIR calibration. Data for (2.2) with $[HO_2]_0 / [C_2H_5O_2]_0 > 1$ (typically 3 different conditions) were then fit in order to approximate k_2. Secondary chemistry from (2.3) does not interfere when HO_2 is in excess because k_2 is ~50 times larger than k_3, and almost all $C_2H_5O_2$ will react with HO_2. The estimate for k_2 was then used in fits of the (2.3) data to give values for k_3 and the branching fraction α.

The values for k_3 and α were then used to fit the rest of the (2.2) data where $[HO_2]_0 / [C_2H_5O_2]_0 < 1$. Under these conditions the secondary chemistry of (2.3) has an effect on the values obtained for k_2. A new value of k_2 was obtained by averaging the values from all of the fits of (2.2) data. This value of k_2 was then used in subsequent fits of data on reaction (2.3), and all of the values were refined iteratively. In practice two iterations were sufficient to achieve convergence. **Table 2-1** presents the full chemical model used while fitting the reactions and what parameters were fit. All fits were performed using the program FACSIMILE.[29]

Data fitting started at 200 μs after the photolysis laser pulse for both reactions. The (2.2) data were typically fit to 5–10 ms. The data for the slower (2.3) were fit out to two half lives (50–200 ms) in order to account for the varying values of $[C_2H_5O_2]_0$. In all fits the radical source chemistry was neglected and the initial radical concentrations $[HO_2]_0$ and $[C_2H_5O_2]_0$, were fit as well. The initial radical concentrations from the fits were consistent with the ratios of $[CH_3OH]$ and $[C_2H_6]$, the precursors of HO_2 and $C_2H_5O_2$, respectively.

Table 2-1. The chemical model used for fitting HO_2 and $C_2H_5O_2$ system of reactions

Reaction	k_{298}[a]	
$HO_2 + C_2H_5O_2 \longrightarrow C_2H_5OOH + O_2$	5.5×10^{-12}	k_2*
$C_2H_5O_2 + C_2H_5O_2 \longrightarrow 2C_2H_5O_2 + O_2$	3.2×10^{-14}	k_{3a}*
$\longrightarrow C_2H_5OH + CH_3CHO$	7.8×10^{-14}	k_{3b}*
$C_2H_5O_2 + O_2 \longrightarrow HO_2 + CH_3CHO$	1.0×10^{-14}	k_4†
$HO_2 + HO_2 \xrightarrow{M} H_2O_2 + O_2$	1.7×10^{-12}	k_5*
$C_2H_5O_2 + C_2H_5O \longrightarrow C_2H_5OOH + CH_3CHO$	1.5×10^{-11}	k_{12}*
$C_2H_5O_2 \xrightarrow{\text{diffusion, UV}}$	$5\ s^{-1}$	k_D*
$HO_2 \xrightarrow{\text{diffusion, UV}}$	$5\ s^{-1}$	k_D‡

[a] units of cm^3 $molecules^{-1}$ s^{-1} except where explicitly written, * determined during this study, † ref [31], ‡ used $C_2H_5O_2$ value

Sample fits with residuals for both (2.2) and (2.3) are shown in **Figure 2-1 A**–**D**. In **A** and **B** are the data and fits for (2.2) at 273 K, 50 Torr, and $[HO_2]_0 / [C_2H_5O_2]_0 = 1.13$ in the NIR and UV, respectively. The high signal-to-noise ratio for the HO_2 NIR signal reveals the subtle systematic residual attributed to diffusion and described in the calibration of the NIR probe portion of the experimental section. Panels **C** and **D** show the NIR and UV traces for reaction (2.3) taken at 273 K, 50 Torr, and 8.8×10^{13} molecules cm^{-3} total radicals. At the HO_2 concentrations in **C** (~100 times lower than **A**) the diffusion effect is masked by the signal noise. For both (2.2) and (2.3) the fits agree well with the UV and NIR signals.

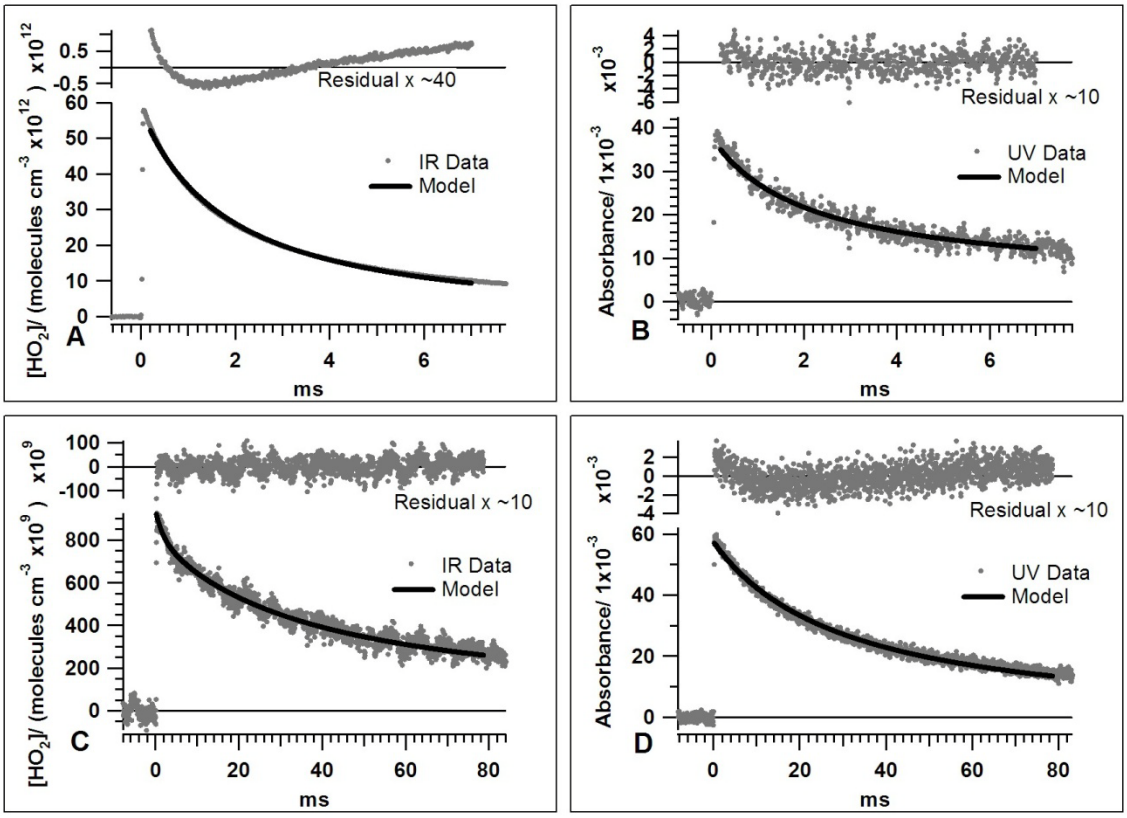

Figure 2-1. (A) Example fit of IR data for reaction (2.2). (B) Example fit of UV data for reaction (2.2). The data were taken at 273 K, 50 Torr, $[CH_3OH] = 4 \times 10^{15}$ molecules cm^{-3} and $[C_2H_5O_2]_0 / [HO_2]_0 = 1.13$. (C) Example fit of IR data for reaction (2.3). (D) Example fit of UV data for reaction (2.3). The data were taken at 273 K, 50 Torr, and $[C_2H_5O_2]_0 = 8.8 \times 10^{13}$ molecules cm^{-3}.

By setting the monochromator to 250.0 nm, the ratio of $C_2H_5O_2$ and HO_2 cross sections was maximized at ~ 10:1 ($C_2H_5O_2$: $\sigma = 4.1 \times 10^{-18}$ cm^2; HO_2: $\sigma = 0.48 \times 10^{-18}$ cm^2)[31] within the operating range of the lamp. The peroxide products of (2.2) and (2.5), C_2H_5OOH and HOOH, respectively, also absorb at 250 nm. The absorption cross section for C_2H_5OOH has not been measured, but was assumed to be the same as that for CH_3OOH. We make this assumption because the hydroperoxides all share a broad dissociative transition in the UV (210–365 nm) due to the breaking of the O-O bond.[32] While σ_{250} for HOOH and CH_3OOH vary by a factor of 2, the values for CH_3OOH and $HOCH_2OOH$ are virtually identical, suggesting that differences past the alpha atom will

not have a large influence on σ. The values used for HOOH and C_2H_5OOH at 250 nm are $\sigma = 8.3 \times 10^{-20}$ and $\sigma = 3.98 \times 10^{-20}$ cm^2, respectively.[31]

The uncertainties stated in the following sections come from random error and systematic error. The random errors are accounted for in a straightforward way by determining the standard deviation from the mean. The mean was determined by averaging values of k_2, k_3, and α from runs at the same temperature and pressure but with different initial radical ratios or total radical concentrations, respectively. One potential source of systematic error was the uncertainty from the fitting procedure just described. In the initial fits to the data for (2.2) where $[HO_2]_0/[C_2H_5O_2]_0$ was high, the low signal-to-noise ratio in the UV detection of $C_2H_5O_2$ and the small systematic residual in the NIR detection of HO_2, led to a range of acceptable fits and a range in the value for k_2. The quality of the fits was determined by the overall residual sum of squares as well as by visual evidence of non-random residuals. The high and low values for k_2 were then propagated through the fitting routine in order to determine the effect of this uncertainty on the values of k_3 and α. The values of k_3 and α returned, but not the overall quality of the fits, relied on the value of k_2 used to fit them. This meant a wide range of k_2 values led to similarly high quality fits to the data from (2.3), but returned a proportionally wide variety in values for k_3 and α. The uncertainty in the k_2 fits and the correlating uncertainties in k_3 and α were smaller than the random uncertainties but not negligible. Both sources of error were combined in quadrature. An example of these 1 σ error bars at two temperatures for k_2 are shown in **Figure 2-2**, and show how the overall uncertainties get larger at $[HO_2]_0/[C_2H_5O_2]_0 > 1$ due to increased uncertainty in the fits.

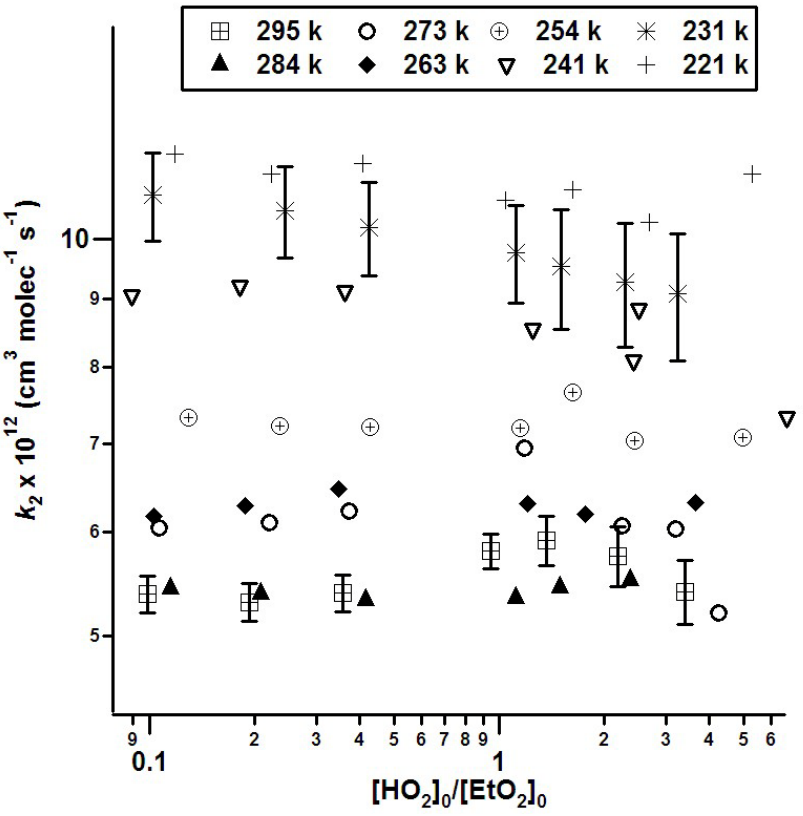

Figure 2-2. Plot of k_2 vs. $[C_2H_5O_2]_0$: $[HO_2]$ for T 221-296 K. Error bars are examples of data precision.

The major source of systematic error was the uncertainty in the path length due to the mixing of the purge and reactant gas flows. The data was analyzed at the maximum and minimum lengths, i.e., 138 and 159 cm, to determine the error associated with this uncertainty. Upper and lower error bounds were determined by applying the random and fitting uncertainties just discussed to the analysis done at the long and short path length. The total error determined in this way was considered a 2σ error bar. The final errors are reported as half this at their 1σ limits. These are the error bars displayed with data presented in **Figure 2-4**, **2-5**, and **2-6**, and in **Table 2-3** and **2-4**. The uncertainties do not take into account the error associated with σ for HO_2 and $C_2H_5O_2$ in the UV.

Another potential contributor to the error from reaction (2.3) is the correlation between parameters k_3 and α. Unlike the correlation between k_2, k_3, and α just described, k_3 and α are impossible to determine independently in this experiment. Fortunately the quality of the fit to the data degrades rapidly if k_3 or α is fixed away from their simultaneously fit values. This meant that the contribution to the overall error was much smaller than the random error and was not included. **Figure 2-3 A**–**B** compares fits that use the JPL-06 ($\alpha = 0.6$), the data fit ($\alpha = 0.28$), and an arbitrary lower value ($\alpha = 0.10$) for α, and provides an example of how fits to the data do not capture the behavior observed when k_3 and α are not fit simultaneously. The NIR HO_2 data in **A** shows clearly that the JPL-06 value for α predicts larger concentrations of HO_2 than are observed, and that the lower value predicts much lower concentrations. In **B** the fit to the UV data that largely determines k_3 shows a much slower rate constant for the JPL-06 and a faster one for the lower α value. **Figure 2-3** demonstrates that although k_3 and α are correlated, pulling one away from its best fit value also pulls the other away from its best fit.

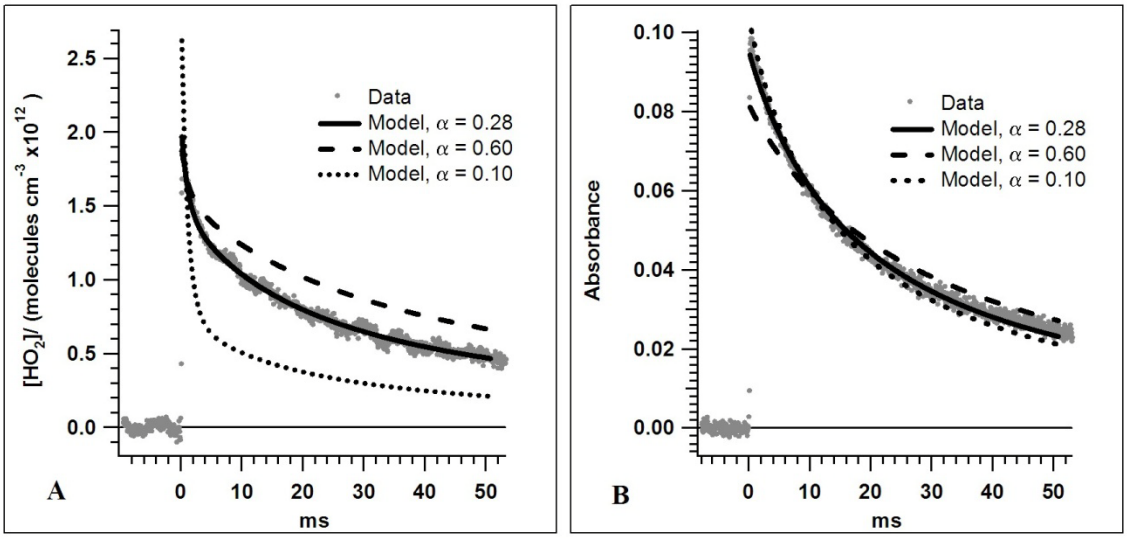

Figure 2-3. (A) Example of NIR data for reaction (2.3) while holding α at three different values, and the effect it produces on the fit. (B) The corresponding UV data.

2.3.3 $HO_2 + C_2H_5O_2$ rate constant

Measurements of the rate coefficient k_2 were performed over the temperature range 221–296 K and the pressure range 50–200 Torr. For each combination of temperature and pressure, the initial radical ratio ($[HO_2]_0 / [C_2H_5O_2]_0$) was varied over the range 0.1–3. The range of initial radical concentrations were as follows, in units of molecules cm^{-3}: $[HO_2]_0 = (0.1\text{-}1) \times 10^{14}$ and $[C_2H_5O_2]_0 = (0.3\text{-}1) \times 10^{14}$. **Figure 2-2** shows the values obtained for k_2 vs. $[HO_2]_0 / [C_2H_5O_2]_0$ at each temperature at a pressure of 50 Torr. For clarity error bars have only been included for 295 K and 231 K. **Figure 2-4** shows a comparison of the current work to previous studies at temperatures < 298 K.

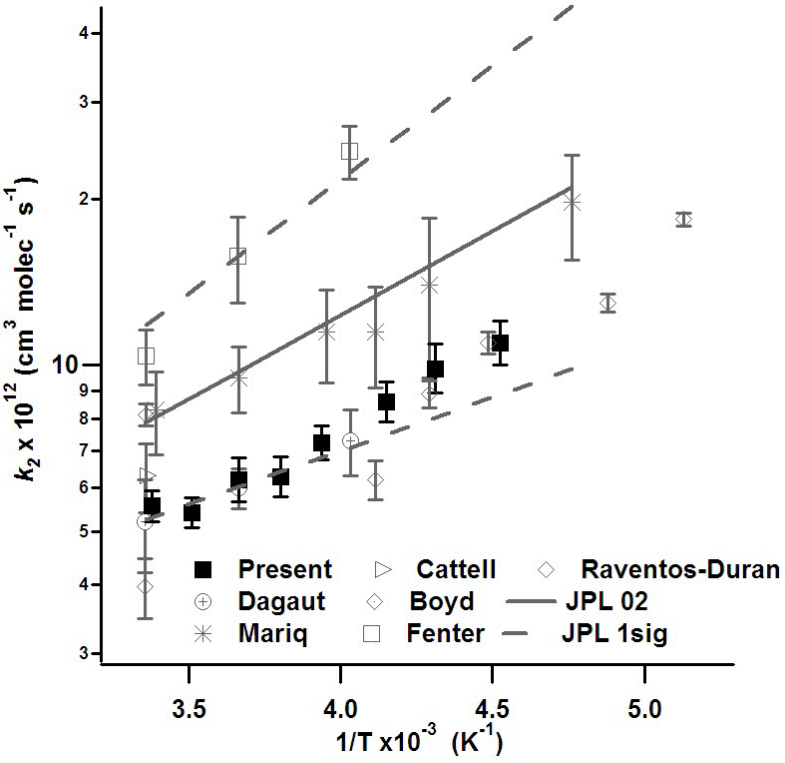

Figure 2-4. Comparison of k_2 with previous work. Error bars are 1σ.

Table 2-2 lists the values of k_2 measured in this study. The values of $k_2(298K)$ and the Arrhenius parameters for all of the studies are given in **Table 2-3**.

Table 2-2. Measured rate constant values for HO2 + $C_2H_5O_2$

T (K)	k_2 / 10^{-12} (a)
295	5.57 ± 0.36
284	5.41 ± 0.36
273	6.20 ± 0.59
263	6.29 ± 0.54
254	7.25 ± 0.52
241	8.59 ± 0.74
231	9.87 ± 1.06
221	11.0 ± 1.08

(a) Units cm^3 $molecules^{-1}$ s^{-1}

Table 2-3. Summary of results for the HO_2 + $C_2H_5O_2$ reaction rate constant

Ref.	A/ 10^{-13} (a)	E_a/R (K^{-1})	k_2(298K)/10^{-12} (a)
[5]	NA	NA	6.3
[6]	5.6 ± 2.4	650 ± 125	5.2
[7]	1.6 ± 0.4	1260 ± 130	10.4
[8]	6.9 (+2.1, -1.6)	702 ± 69	8.3
[4]	NA	NA	8.14
[9]	2.08 (+0.87, -0.62)	864 ± 79	3.97
(b)	**6.01 (+1.95, -1.47)**	**638 ± 73**	**5.6**

(a) Units $molecules^{-1}$ cm^3 (b) Current study

An Arrhenius fit to our data gives, $k_2(T) = \left(6.01\ ^{+1.95}_{-1.47}\right) \text{x} 10^{-13} \exp\left(\frac{638 \pm 73}{T}\right)$. The pressure dependence of k_2 was studied over the range 50–200 Torr of N_2 at 296 K and 231 K. No dependence on pressure was observed at either of these temperatures in agreement with previous measurements.[5,6,8,9]

2.3.4 $C_2H_5O_2 + C_2H_5O_2$ kinetics and branching fraction

Three kinetics parameters were determined from the studies of (2.3): k_{3obs}, k_3, and α. Reaction (2.3) was investigated over the same temperature range as (2.2), 221–296 K. The total initial radical concentration was varied over the range 3.0 x 10^{13}–1.5 x 10^{14} molecules cm^{-3}. At the largest total radical concentrations O_2 was varied to check for secondary chemistry other than the production of HO_2. Using the UV data alone it is possible to determine k_{3obs} which is related to k_3 by equation (i). The value of k_{3obs} measures the total loss of $C_2H_5O_2$. It incorporates loss from both the self reaction and from reaction with secondary HO_2. Combining the UV and NIR data allows for determination of k_3 and α. Values for k_{3obs} were measured over the pressure range 50–200 Torr. Values for k_3 and α could only be measured at 50 Torr because of decreased sensitivity due to pressure broadening in the WM detection of HO_2.

It is difficult to directly compare the different values of k_{3obs} from different studies because the value actually measured, k_{3obs}/σ_λ is dependent on the wavelength used to make the determination and the spectrometer instrument lineshape function. In the present study to determine k_{3obs}, λ = 250 nm was used and σ_{250} was taken from the JPL-06 recommendation.[31] In order to compare with the present work, previous data sets were normalized to the value of σ recommended in the JPL-06 evaluation for the λ used in that experiment. **Figure 2-5** compares the previous and present work on k_{3obs}.

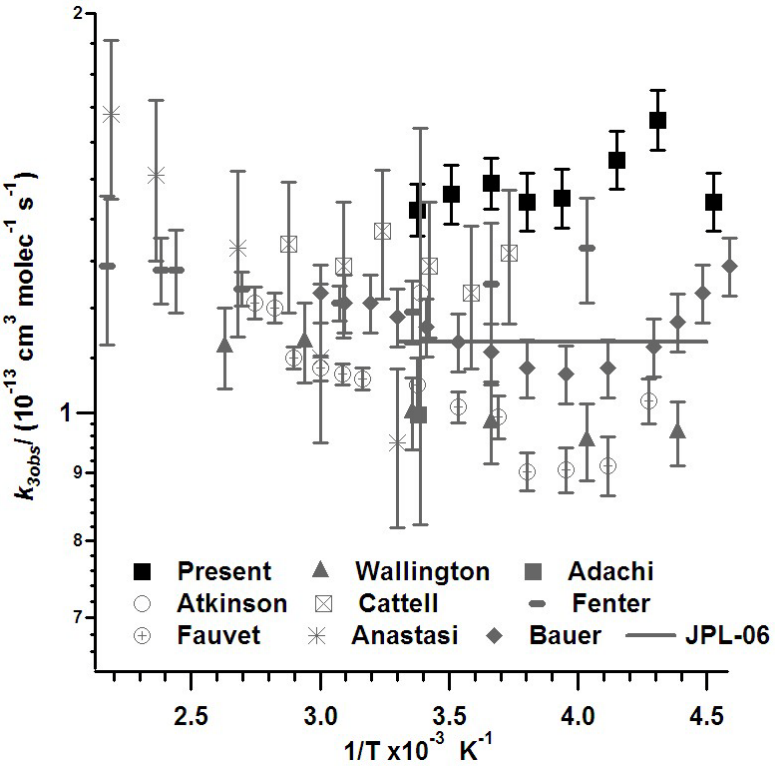

Figure 2-5. Comparison of k_{3obs} with previous work. Error bars are 1 σ.

An Arrhenius fit to our data leads to the expression

$k_{3obs}(T) = \left(1.18\ ^{+0.23}_{-0.19}\right) \text{x} 10^{-13} \exp\left(\frac{58 \pm 45}{T}\right)$. **Table 2-4** presents our data for k_{3obs} at all temperatures and pressures . We do not see a pressure dependence for k_{3obs} in agreement with previous results, however there is a slightly anomalous decrease in k_{3obs} at 200 Torr. Values for k_d, the rate constant for the unimolecular disappearance due to diffusion were determined along with the values for k_{3obs}. For $C_2H_5O_2$, $k_d = 5 \pm 1$ s^{-1} and was invariant over the pressure range 50–200 Torr. Diffusion constants should be inversely proportional to pressure, so if rather than using the measured value we assume a linear dependence on pressure (i.e., if $k_d = 5$ s^{-1} at 50 Torr then at 200 Torr $k_d = 1.25$ s^{-1}) and use that to fit the 200 Torr data we get values for k_{3obs} that agree much better. These values are shown in parenthesis for the 200 Torr data in **Table 2-4**. While it can not be ruled out

that the lower pressure data are under-representing the diffusion effect, this seems unlikely because the fits to the 200 Torr data improve based on total residual sum of squares when using the lower k_d values. Trying the opposite route, increasing k_d for the 50 Torr data linearly (i.e., 50 Torr k_d = 20 s^{-1}) from the fitted 200 Torr values, leads to unacceptable fits.

Table 2-4. Results of $C_2H_5O_2$ self reaction at all temperatures and pressures

T (K)	P (Torr)	k_{3obs} / 10^{-13} (a)	k_3 / 10^{-13} (a)	α
295	50	1.42 ± 0.07	1.10 ± 0.09	0.32 ± 0.05
284	50	1.46 ± 0.08	1.17 ± 0.07	0.27 ± 0.03
273	50	1.49 ± 0.07	1.22 ± 0.05	0.23 ± 0.03
263	50	1.44 ± 0.07	1.18 ± 0.06	0.23 ± 0.03
254	50	1.45 ± 0.08	1.13 ± 0.06	0.30 ± 0.03
241	50	1.55 ± 0.08	1.24 ± 0.07	0.28 ± 0.03
231	50	1.66 ± 0.09	1.36 ± 0.11	0.25 ± 0.05
221	50	1.44 ± 0.07	1.02 ± 0.07	0.43 ± 0.05
295	200	1.20 ± 0.09 (1.55)		
231	200	1.23 ± 0.09 (1.62)		
298[b]	all P	1.1	6.8	0.6

(a) Units cm^3 $molecule^{-1}$ s^{-1}. (b) Values from [1]

The values for α are shown in **Figure 2-6** along with the previous results from the end product studies. To our knowledge this is the first published investigation of the temperature dependence of α below room temperature. A weighted average of the measurements leads to the expression α = 0.28 ± 0.06. The larger error bars and scatter of the measured value reflect the sensitivity of α to correlation with the other parameters, but were not interpreted as any temperature dependence.

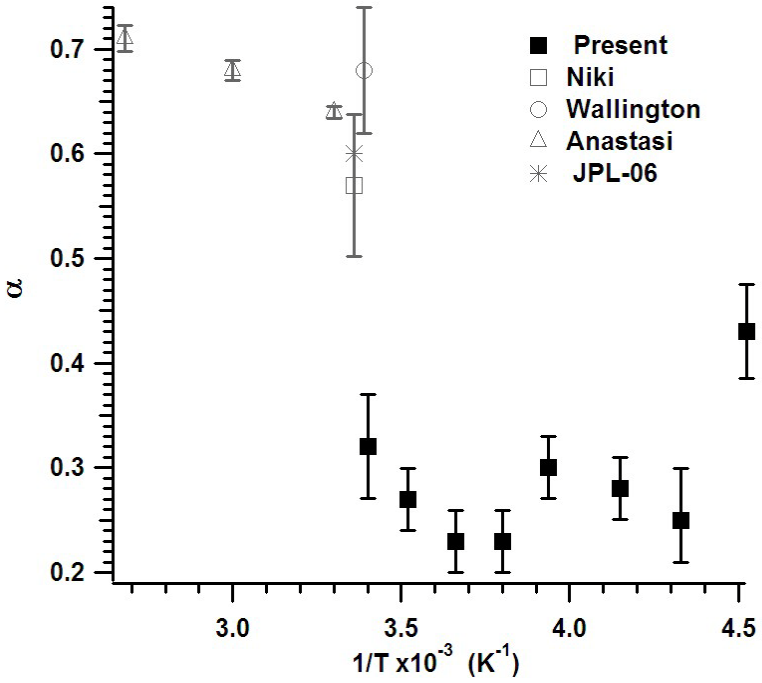

Figure 2-6. Comparison of α with previous work. Error bars are 1σ.

For reaction (2.3) varying the $[O_2]$ provided a check on whether (2.4) was the only subsequent reaction of C_2H_5O. In our experiments where $[O_2]$ was varied no difference in k_{3obs} was measured similar to the experiments of Cattell et al.[5] However values for α did not remain consistent as $[O_2]$ varied, and the temporal profile of HO_2 from the IR data could not be fit as accurately. Inclusion of the chemistry suggested by Cattell et al.,

$$C_2H_5O + C_2H_5O_2 \longrightarrow C_2H_5OOH + CH_3CHO" \qquad (2.12)$$

allowed for agreement across all $[O_2]$ values. Values for k_{12} were generally determined at the lowest $[O_2]$ values where (2.4) would be slowed. The rate coefficient k_{12} = (1.54 ± 0.7) x 10^{-11} cm^3 $molecules^{-1}$ s^{-1} independent of temperature.

Lastly it was possible to measure k_3 directly. The Arrhenius expression derived from the data is, $k_3(T) = \left(1.29\ ^{+0.34}_{-0.27}\right) \text{x} 10^{-13} \exp\left(\frac{-23 \pm 61}{T}\right)$. **Table 2-4** shows the values measured for k_{3obs}, k_3, and α along with current recommendations for them.

2.3.5 CH_3OH Chaperone effect

The methanol chaperone effect on (2.5) has previously been investigated in this laboratory and others.[12,13] This effect enhances the observed rate of reaction at low temperatures through the following mechanism.

$$HO_2 + CH_3OH \rightleftharpoons HO_2 \bullet CH_3OH \quad (2.13)$$

$$HO_2 + HO_2 \bullet CH_3OH \longrightarrow H_2O_2 + CH_3OH + O_2 \quad (2.14)$$

$$\text{Net: } HO_2 + HO_2 \xrightarrow{CH_3OH} H_2O_2 + O_2 \quad (2.15)$$

Under the conditions of low [CH_3OH] used in this experiment, the dependence of k_{5obs} on [CH_3OH] is that derived in the Christensen et al. paper,[33]

$$k_{5obs} = k_5 + (k_{14} - 2k_5) K_{13} [CH_3OH] \quad \text{(iii)}$$

In this experiment it was investigated whether the HO_2•CH_3OH complex might change the observed kinetics of (2.2). At 241 K, a set of experiments at [CH_3OH] of 1×10^{15}, 2.5×10^{15} and 5×10^{15} molecules cm^{-3} were performed. No evidence for a methanol chaperone effect was observed on (2.2) at the conditions studied. We were unable to investigate this effect further at lower temperatures and/or higher [CH_3OH] due to the large amount of complex that is formed under those conditions. When > ~10% of the HO_2 exists in a complexed state the UV and NIR spectroscopy in this experiment are no longer observing the same simple bimolecular reaction. This makes it difficult to

accurately calibrate the NIR probe signal. A comprehensive study including other temperatures below 298 K as well as looking at the effect of H_2O would be valuable, but was outside the scope of the present work.

2.4 Discussion

The major strength of this experiment was the ability to monitor HO_2 and $C_2H_5O_2$ using simultaneous but distinct optical probes in the NIR and UV, respectively. A self consistent method was used for measuring the interrelated parameters k_2, k_3, and α. For the first time α was determined by measurement of the nascent radical product on the time scale of the reaction.

There are a number of experimental concerns that need to be addressed when looking at the self and cross reactions of HO_2 and $C_2H_5O_2$, or any RO_2 for that matter. In the cross reaction (2.2) it is important to investigate a wide range of initial radical ratios ($[HO_2]_0/[C_2H_5O_2]_0$) to test for consistency in the results. The simplest conditions to investigate (2.2) are where (2.3) is suppressed, i.e., at $[HO_2]_0/[C_2H_5O_2]_0 > 1$. This prevents interference due to secondary production of HO_2 from (2.4), and leaves (2.5) as the only competing pathway to (2.2). Experiments done under the conditions of the more complicated case where $[HO_2]_0/[C_2H_5O_2]_0 < 1$, must carefully consider the secondary chemistry of (2.3) and (2.4). Under these conditions measurements of k_2 also implicitly check the parameters used for (2.3) due to their influence on the observed rate coefficient. **Figure 2-2** shows the wide range of initial radical ratios examined in the current study of (2.2), and the good agreement across these conditions. The initial radical ratio varied from ~ 0.1–4 at all temperatures. This range is considerably wider than employed in previous studies. As initial conditions shift to more $C_2H_5O_2$ and the secondary chemistry

plays a larger role, the value of α used influences what value of k_2 is determined by the model.

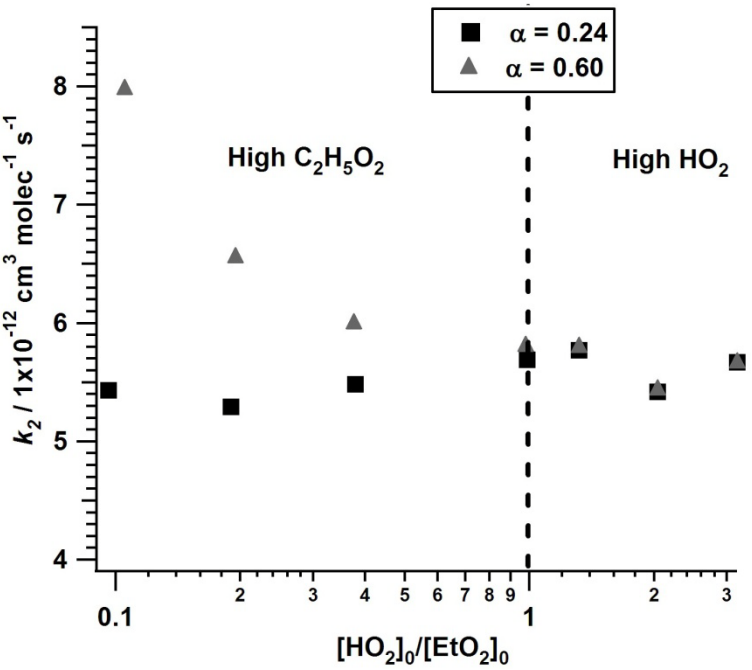

Figure 2-7. Comparison of the fitted values for k_2 using either the previous recommendation for α or the value measured in this study

Figure 2-7 shows the dependence of k_2 on $[HO_2]_0/[C_2H_5O_2]_0$ and α. The data shown are the same except that the value for α used in the model fits was fixed at either the literature value of 0.60, or the value measured by this experiment of 0.24. Prior to performing the current measurement of α we could not explain the trend observed of increasing k_2 with decreasing $[HO_2]_0/[C_2H_5O_2]_0$. Our lower values for α led to a consistent value for k_2. This made it clear that previously the model was trying to compensate for too much secondary HO_2 by increasing the rate of loss of HO_2 by (2.2). **Table 2-5** (given at the end of the chapter) lists the initial radical ratios explored by the previous temperature-dependent studies of (2.2). **Figure 2-7** shows that examining a wide range of initial radical ratios provided a useful check on the consistency of the results.

Another issue that is important to look at is the use of CH_3OH as a precursor for HO_2 in (2.2). CH_3OH is a common precursor for HO_2, but, as discussed in the results and analysis section, it is now known that CH_3OH and HO_2 form a hydrogen bonded complex at low temperatures that enhances the observed rate of the HO_2 self reaction (2.5). Previous studies that used CH_3OH as a precursor may have underestimated k_5 because the chaperone effect was not accounted for. This may have led to an overestimate of k_2 in order to fit the observed time decay of the HO_2 signal, thus attributing the increased decay to reaction with $C_2H_5O_2$ instead of the effect of $CH_3OH \bullet HO_2$ on (2.5). In the section on comparison with previous work it will be noted when this could be a contributing factor. This experiment does not see a direct enhancement in the observed rate coefficient k_2 due to the $CH_3OH \bullet HO_2$ complex reacting with $C_2H_5O_2$. Therefore it is only the chaperone effect on k_5 that could cause problems.

The last experimental issue pertains to the measurement of α. This experiment is able to make the first direct measurement on the time scale of the reaction. The other studies have all relied on ratios of stable end products minutes after the reaction, which are susceptible to unknown production mechanisms.

2.4.1 Previous work: $HO_2 + C_2H_5O_2$

Figure 2-4 displays the all of the previous work on reaction (2.2) at temperatures < 298 K. The present work is in closest agreement with Dagaut et al.[6] As with all of the UV absorption studies, Dagaut et al. was not able to independently monitor both radicals, but had to rely on spectral deconvolution. The study also only looked at two temperautures below 298 K. Three other factors that may influence the agreement between the studies are: the initial radical ratio range explored, the use of CH_3OH as an

HO_2 precursor, and the UV cross section used. Dagaut et al. did explore a wide range of initial radical ratios, but they were using the larger value for α recommended by the end product studies. This may have biased their results to larger values although they did not report any discrepancy in k_2 when changing initial radical ratio. They also used large values of CH_3OH (1.1–5.5 x 10^{16} molecules/cm^3) as an HO_2 precursor without accounting for the CH_3OH chaperone effect, leading to a potential overestimate of k_2 at lower temperatures. Lastly, the UV cross sections used by Dagaut et al. were lower than those currently recommended and it is estimated that using the current recommendation would add ~20–30% to the values reported.[2,8] It is possible that the competing errors may somewhat offset each other, leading to the agreement seen.

Maricq et al.[8] is another UV absorption study in reasonable agreement with our work. The study used fluorine chemistry as a precursor for its radicals so no correction for CH_3OH is needed. There is good agreement for the value of $\frac{E_A}{R}$ across Dagaut et al., Maricq et al., and the current work. Some of the difference between the actual values in Maricq et al. and the present work can probably be attributed to larger k_2 from larger α values used because the bulk of their experiment were carried out at $[HO_2]_0/[C_2H_5O_2]_0$ = 0.67. However, the small excess of $C_2H_5O_2$ under their conditions would account for at most 5–10% of the ~50% discrepancy. There are no other obvious reasons for the discrepancy between the experiments, but especially at low temperatures the agreement becomes better as the data sets agree within the stated uncertainties.

Fenter et al.[7] is the temperature dependent study that deviates from the rest. It was a UV absorption study similar to the Maricq et al. and Dagaut et al. work. The low

temperature data were limited to two points below 298 K, and the study also used large CH_3OH concentrations (1.5–6 x 10^{16} molecules/cm^3) without knowing about the chaperone effect. This effect would not be large enough to account for the discrepancy seen here. As has been stated previously, there is no clear reason for the discrepancy between the Fenter et al. results and the rest.[8] The Arrhenius parameters and k_2(298K) of Fenter et al. stand out in **Table 2-3.** The results from the present study and Raventos-Duran et al. suggest that there may have been systematic errors in the low temperature data of Fenter et al.

The most recent investigation is the Raventos-Duran et al.[9] work, which used the CIMS technique. This experiment was the only one not using UV absorption for radical detection, and was the first temperature-dependent study to independently monitor the HO_2 and $C_2H_5O_2$ concentrations. The agreement between the Raventos-Duran et al. work and the current study appears acceptable especially at low temperatures. Their $\frac{E_A}{R}$ value of 864 K^{-1} is slightly larger than the currently recommended value of 700 K^{-1}.

There have also been two room temperature studies by Cattell et al. and Boyd et al.[4,5] The Cattell et al. study was the first to use diode laser IR spectroscopy to independently monitor HO_2. They could not simultaneously measure HO_2 and $C_2H_5O_2$, as in the current study, but there is good agreement between our values. The Boyd et al. study used only UV absorption and is in better agreement with the Maricq et al. value at 298K.

Overall the present work is part of a convergence in the measurements of k_2. The largest uncertainties remain in its 298 K value, but there is agreement in its temperature dependence and overlap among lower temperature data points within their uncertainties.

2.4.2 Previous work: $C_2H_5O_2 + C_2H_5O_2$: k_{3obs}

All previous investigations of reaction (2.3) have either studied the kinetics or the branching fraction of the reaction, but unlike this experiment, never both simultaneously. Previous kinetics measurements obtained values for k_{3obs} and then determined k_3 using α determined from end product studies and the relationship in equation (i). **Figure 2-5** is a comparison of results for k_{3obs}. The results from this study are the largest reported values and are ~25% larger than the JPL-06 recommended value at 298 K. We report an $\frac{E_A}{R}$ = -58 K by fitting an Arrhenius expression to the data. Of the previous studies, The Fenter et al.[7] work ($\frac{E_A}{R}$ = -60 K) and the Cattell et al.[5] data ($\frac{E_A}{R}$ ~ 0) are in the closest agreement with the present study. The Fauvet et al.[17] ($\frac{E_A}{R}$ = 128 K) and Wallington et al.[19] ($\frac{E_A}{R}$ = 110 K) agree very well with each other and both observe the opposite trend of a steady decrease in rate constant with temperature. Anastasi et al.[11] also observed a decreasing rate constant but with a much steeper decline than was observed in any other study. None of the other previous studies went quite as low in temperature as Bauer et al. so it is possible that they would not have observed the change in temperature dependence observed by Bauer et al., and there is some evidence for the beginning of a change at the lowest temperature of Wallington et al. and Fauvet et al. There are no clear experimental reasons for the discrepancies between the different studies. All the studies were done using UV absorption, and the data have been normalized as best possible for differences in σ as discussed in the results section. **Table 2-6** (given at the end of the chapter) summarizes the experimental conditions of each study and the measured $\frac{E_A}{R}$. Agreement

between studies is not split down obvious lines of different experimental techniques, source chemistry, or pressure range. None of the previous studies saw any effect due to pressure. The overall spread in the data from the different studies would ideally be less, but is not unreasonable. However the temperature dependence of the reaction is still very uncertain and more work to determine it is needed.

2.4.3 Previous work: $C_2H_5O_2 + C_2H_5O_2$: k_3 and α

This experiment is the first to measure k_3 directly, and not rely on equation (i) in order to calculate it. **Table 2-4** lists the values measured and compares then with the current recommendation.[31] The measured values are nearly twice the currently recommended value. This increase is predominantly due to the difference in α as the relationship in equation (i) is a valid approximation for most conditions. The rest of the discrepancy is explained by the slightly larger values of k_{3obs} discussed above. The current recommendation lists (2.3) as having no T dependence which is in agreement with the value from this work, $\frac{E_A}{R} = 23 \pm 61$.

The current study is also the first "direct" study of α. Monitoring the HO_2 from reaction (2.4) is not technically a direct measurement as it is one step removed from the actual $C_2H_5O_2$ self reaction. However under most experimental conditions sufficient O_2 insured essentially complete conversion by reaction (2.4) and the possibility of (2.12) was accounted for. Every previous measurement of α was a continuous photolysis end product study which made measurements of the stable products on a timescale of minutes. Of the five previous studies on α we will focus on three.[11,21,22] The other works by Kaiser et al.[20] and Anastasi et al.[14] were superseded by a new study from the same

group and never published in the peer reviewed literature, respectively, and so will not be mentioned further here. **Figure 2-6** shows the wide gap between the current and previous measurements, this discrepancy is discussed below.

The study by Anastasi et al.[11] was a continuous photolysis experiment using azoethane ($(C_2H_5)_2N_2/O_2$) initiation chemistry and irradiation by UV lamps. They used GC/MS detection of the products over the course of minutes and explored temperatures in the range 303–372 K. Total pressure was varied, but typically was ~500 Torr. Product ratios were related to the reaction rates by the expressions:[21]

$$\left[C_2H_5OH\right]/\left[CH_3CHO\right] = k_{3b}/\left(2k_{3a} + k_{3b}\right) \quad \text{(iv)}$$

$$\left[C_2H_5OOH\right]/\left[C_2H_5OH\right] = 2k_{3a}/k_{3b} \quad \text{(v)}$$

They also explored the effect different O_2 concentrations had on the product ratios, and noticed an increase in C_2H_5OOH yield and decrease in C_2H_5OH yield as O_2 is raised. This indicates that the products in reaction (2.12) may not only be the stable ones suggested, but instead may also have a channel producing C_2H_5OH and a diradical (e.g., CH_3CHOO). Overall they did not observe steady product ratios over time and tried to rely on the initial rates of formation at high O_2 to determine α. In the modeling of their data they also used quite different values for key rate coefficients which could have influenced their determination of the initial rates. The combination of these effects makes it difficult to compare their results to the current study, but does suggest that it's possible that the different timescales of the end product study and the current study could display very different results.

The first measurement of α was made by Niki et al.[21] using a continuous photolysis FTIR experiment at room temperature and 700 Torr. Data were typically

recorded after 5,10, or 20 min periods of irradiation by UV lamps. Both azoethane and chlorine ($Cl_2/C_2H_6/O_2$) chemistries were used to generate the radicals. Similar product ratios for $[C_2H_5OH]/[CH_3CHO]$ were found for both chemistries and there was no change over time. A different ratio than those previously mentioned, the ratio of $[C_2H_5OOH]/[CH_3CHO]$ did appear to decrease with time, and this decrease was more evident when using the azoethane chemistry that required longer irradiation times. They interpreted the changing ratio as a heterogeneous loss of C_2H_5OOH. One possibility of chemistry that was overlooked in this study is the reaction of Cl with C_2H_5OH.[34]

$$Cl + C_2H_5OH \longrightarrow \text{products} \qquad (2.16)$$

$$\longrightarrow CH_3CHOH + HCl\ (90\%) \qquad (2.16a)$$

$$\longrightarrow CH_2CH_2OH + HCl\ (10\%) \qquad (2.16b)$$

$$CH_3CHOH + O_2 \longrightarrow HO_2 + CH_3CHO \qquad (2.17)$$

If this chemistry were occurring in the chlorine system then it could provide an explanation for how, over time, the yield of C_2H_5OH could be artificially reduced and that of CH_3CHO increased to yield an apparently higher branching fraction in k_{3a}. Simultaneous Cl reaction with CH_3CHO at comparable rates as (2.16) would keep the ratio in equation (iv) stable,[35,36] as observed in their data. However this chemistry would not explain the agreement seen between the two different initiation chemistries because this chemistry would not occur in azoethane mixture where no Cl is present.

The last study by Wallington et al.[22] is very similar to the Niki et al. study, and is also a continuous photolysis FTIR study. It was a room temperature study at 700 Torr total pressure. Chlorine initiation chemistry was used and no change in the product ratios with time was observed. They note that they had the smallest surface/volume ratio of any

of the previous experiments, minimizing the effect of any surface reactions. The reactions of Cl with the products C_2H_5OH, CH_3CHO, and C_2H_5OOH were modeled and corrections were made to the observed product ratios, but it does not appear that the full sequence of reactions (2.16) – (2.17) are included, allowing another route of production for CH_3CHO. For both the Niki et al. and Wallington et al. studies there are no clear reasons for the discrepancy between the current results and theirs.

One hypothesis for the discrepancy between the end product studies and the current one is the pathway (2.3c) and then photolysis of the diethylperoxide $C_2H_5O_2C_2H_5$.

$$C_2H_5OOC_2H_5 \xrightarrow{h\nu} 2C_2H_5O \qquad (2.18)$$

Of the three studies only Niki et al. saw any evidence for its formation. If the diethylperoxide formed and photolyzed on the timescale of seconds it would generate ethoxy radicals. The ethoxy radicals would not be distinguishable from the fraction of the reaction that proceeded through pathway (2.3a) and would be lumped together during the end product studies.

The lower value of α measured in this study is closer in value to α for the CH_3O_2 self reaction, which ranges from 0.28–0.43.[2] Agreement would not necessarily be expected because k_{3obs} for CH_3O_2 is 3–4 times larger than for $C_2H_5O_2$ indicating that different pathways may be preferred in each case.[2] It is also interesting that a temperature dependence is not observed for α in this study. An experiment by Horie et al.[37] on CH_3O_2 suggest that there is a steep decrease in the k_{3a}/k_{3b} branching ratio with temperature down to 223 K. The overall temperature dependence of (2.3) is fairly flat in the studied temperature range, unlike the behavior seen in the CH_3O_2 self reaction rate coefficients, which may explain some of the observed difference between the two systems. Still α

could easily have a temperature dependence due to the different barriers for different product channels, while the overall rate coefficient temperature dependence would only be determined by the initial intermediate formation. Given the large deviation between α measured with our experiment and the value from the end product studies in the literature, validation of these results will be necessary.

2.4.4 Mechanism

The complete picture of reaction (2.2) has been developed by work done on both the mechanism and products of the reaction. A number of product studies using FTIR have determined that the product channel shown for reaction (2.2) is the only one available at room temperature.[38-40] The Raventos-Duran et al.[9] temperature-dependent CIMS study confirmed that C_2H_5OOH is the major product channel all the way down to 195 K.[9] Work by Elrod et al. on $CH_3O_2 + HO_2$[41] detected a minor channel leading to the products $HCHO + H_2O + O_2$ that grew larger at lower temperature. The Raventos-Duran et al. work could not check for the analogous minor channel leading to $CH_3CHO + H_2O + O_2$, and so this would be worth investigating. Recent theoretical works agree with the product studies about the dominant product channel,[9,42,43] and are coming to a consensus on the likely mechanism for $RO_2 + HO_2$ reactions in general. The general mechanism involves the formation of both a hydrogen bonded intermediate on the triplet surface and a tetroxide intermediate on the singlet surface. Barriers to the transition state are too high on the singlet surface (when R is a straight chain alkyl group) despite the more stable nature of the tetroxide. The bulk of the reaction then proceeds through the hydrogen bonded structure on the triplet surface. The intermediate formation is indicative of the negative activation energy observed in the reaction's Arrhenius dependence. The lack of

an observed pressured dependence on the reaction indicates that the intermediate formation is the rate limiting step and that it proceeds to products prior to a collision. The fact that collisional stabilization is not needed prior to reaction may explain the lack of an observed enhancement in the rate of reaction (2.2) in the presence of the HO_2•CH_3OH complex, as there is no benefit to having the CH_3OH as a collision partner.

Other HO_2 hydrogen bonded complexes have shown a similar lack of rate enhancement when reacting with RO_2. The HO_2•H_2O complex has been observed and its effect of increasing the observed rate of reaction (2.5) is well known.[44-47] The large amounts of H_2O vapor in the atmosphere make the reactions of HO_2•H_2O potentially very important. Recent work from English et al. showed that H_2O did not enhance the observed rate of reaction between CH_3O_2 + HO_2.[48] This work, along with the current study provides further confirmation of the likely mechanism for the RO_2 + HO_2 reactions.

The mechanism of reaction (2.3) and the self reaction of RO_2 in general needs more work. A recent paper by Dibble et al. nicely summarizes the current theory and its problems.[49] The Russell mechanism for the production of the stable products through a cyclic tetroxide intermediate has been the accepted mechanism for all simple RO_2 self reactions.[50] However, the most rigorous theoretical study on the smallest system, the CH_3O_2 self reaction, did not find a transition state resembling the Russell mechanism pathway.[51] This raises serious questions that need to be resolved given the long standing acceptance of the Russell mechanism. For reaction (2.3) specifically there has been only one computational attempt to determine the reaction pathway.[52] This study shows a transition state below the energy of the reactants for all three reaction paths (R3a–c), but in light of the analysis in the Dibble paper may need a higher level of theory to capture

the behavior observed in experiments. Furthermore, given the uncertainty now in the measured value of α, understanding the actual reaction path to the various product channels will allow a prediction of α to compare with the experiments. Lastly, from the variation in rate constants between the CH_3O_2 and $C_2H_5O_2$ self reactions (~4.5 x 10^{-13} and ~1.5 x 10^{-13}), it is clear that work on different examples of RO_2 are needed to understand the mechanism of the self reaction and shed light on the variety of kinetics measured.

2.5 Conclusion

The kinetics of the $C_2H_5O_2$ reaction system, including k_2, k_{3obs}, k_3, and α, were measured using simultaneous independent detection of the $C_2H_5O_2$ and HO_2 radicals. WM NIR spectroscopy allowed for sensitive and specific detection of HO_2 while UV absorption was used to predominantly monitor $C_2H_5O_2$. The first direct measurements of k_3 and α were made and their sensitivity to k_2 was established. Self consistency established between all the measured parameters provided confidence in the measurements and helped determine the overall uncertainty in each. The experiments on the atmospherically important k_2 added to the growing consensus on the mechanism and overall rate constant for this reaction with an Arrhenius expression $k_2(T) = \left(6.01^{+1.95}_{-1.47}\right) \text{x} 10^{-13} \exp\left(\frac{638 \pm 73}{T}\right)$. Meanwhile the measurements of k_3 and α provided strikingly different results than those obtained previously, $k_3(T) = \left(1.29^{+0.34}_{-0.27}\right) \text{x} 10^{-13} \exp\left(\frac{-23 \pm 61}{T}\right)$ and $\alpha = 0.28 \pm 0.06$ independent of temperature. The difference in α is especially glaring given that its literature value is

frequently used as the branching fraction value for all RO_2 self reactions with $R \neq CH_3$. It was also the first low temperature study of α. Both experimental and theoretical verification of k_3 and α are needed in order to better understand the self reactions of $C_2H_5O_2$ and the self reactions of RO_2 in general.

Table 2-5. Summary of experimental conditions for the determination of the $HO_2 + C_2H_5O_2$ reaction rate constant

Ref	Method[(a)]	Source Gases	$[CH_3OH]$[(b)]	Bath	T[(c)]	P[(e)]	$[EtO_2]_0$:$[HO_2]_0$	λ_{UV}[(f)]
6	FP/UV	$Cl_2/O_2/C_2H_6/CH_3OH$	1.1–5.5	N_2	248–380 298	100 25–400	0.22–6	250
7	FP/UV	$Cl_2/O_2/C_2H_6/CH_3OH$	1.5–6	N_2	248–460	760	0.5–2.0	220 260
8	LFP/UV	$F_2/O_2/C_2H_6/H_2$	--	N_2	210–363	200	1.3 (0.6–2 at 243 and 338 K)	
5	FP/UV/IR	$Cl_2/O_2/C_2H_6/CH_3OH$	0.06	N_2	295	2.4	2	210 260
4	LFP/UV	H_2O_2/C_2H_6	--	air	298	760	0.1–0.25	210 270
9	CIMS	$F_2/O_2/C_2H_6/H_2/He$[(i)]	--	N_2	195–298	75–200	<1	
(h)	LFP/UV/IR	$Cl_2/O_2/C_2H_6/CH_3OH$	0.001–0.1	O_2	221–296	100	0.3–10	250

(a) FP: Flash photolysis, LFP: Laser flash photolysis, CIMS: Chemical ionization mass spectrometry, UV: UV absorption spectroscopy, IR: near-IR diode laser spectroscopy. (b) Units: $\times 10^{16}$ molecules cm^{-3}. (c) Units: K. (e) Units: Torr. (f) Units: nm (h) Current study (i) microwave discharge creates radicals.

Table 2-6. Summary of previous experiments on $C_2H_5O_2 + C_2H_5O_2$

ref	technique	source gas	T (K)	P (Torr)	λ(nm)	$\sigma^a/10^{-18}$ used[b]/rec[c]	E_a/R (K)
10	FP/UV	(CH3CH2)2N2/O2	298	625	230–250 (236)	3.9/4.4	-
11	MM/UV	(CH3CH2)2N2/O2	303–457	495	240	6.23/4.52	?
18	PR/UV	H2/C2H4/O2	298	760	240	5.19/4.52	-
5	MM/UV	(CH3CH2)2N2/O2	266–347.5	27–760	260	3.4/3.24	0
19	FP/UV	Cl2/C2H6/O2	228–380	25–400	250	3.89/4.12	110±40
16	MM/UV	Cl2/C2H6/O2	218–333	760	250	4/4.12	147±30[e]
7	FP/UV	Cl2/C2H6/O2	248–260	760	220–260 (240)	4.89/4.52	-60±40
17	MM/UV	Cl2/C2H6/O2	253–363	200	240–250 (250)	4.04/4.12	128
15	LFP/CRDS	Cl2/C2H6/O2	295	5.5	270	2.14/2.14	-
(d)	LFP/UV	Cl2/C2H6/O2	221–295	50–200	250	4.12/4.12	-58±45

FP: Flash photolysis, MM: Molecular modulation, PR: Pulse Radiolysis, LFP: Laser flash photolysis, UV: UV absorption, CRDS: Cavity ringdown spectroscopy, (a) units of cm^{-2}, (b) value of σ used in the ref. to determine k_{3obs}, (c) value of σ from JPL-06[31] that was used to normalize k_{3obs}, (d) Current study, (e) Over the T range 250–330, below 250 curvature is observed.

2.6 References

(1) Jacob, D. J. *Introduction to Atmospheric Chemistry*; Princeton University Press: Princeton, NJ, 1999.

(2) Tyndall, G. S.; Cox, R. A.; Granier, C.; Lesclaux, R.; Moortgat, G. K.; Pilling, M. J.; Ravishankara, A. R.; Wallington, T. J. *Journal of Geophysical Research-Atmospheres* **2001**, *106*, 12157.

(3) Rudolph, J. *Journal of Geophysical Research-Atmospheres* **1995**, *100*, 11369.

(4) Boyd, A. A.; Flaud, P. M.; Daugey, N.; Lesclaux, R. *Journal of Physical Chemistry A* **2003**, *107*, 818.

(5) Cattell, F. C.; Cavanagh, J.; Cox, R. A.; Jenkin, M. E. *Journal of the Chemical Society-Faraday Transactions Ii* **1986**, *82*, 1999.

(6) Dagaut, P.; Wallington, T. J.; Kurylo, M. J. *Journal of Physical Chemistry* **1988**, *92*, 3836.

(7) Fenter, F. F.; Catoire, V.; Lesclaux, R.; Lightfoot, P. D. *Journal of Physical Chemistry* **1993**, *97*, 3530.

(8) Maricq, M. M.; Szente, J. J. *Journal of Physical Chemistry* **1994**, *98*, 2078.

(9) Raventos-Duran, M. T.; Percival, C. J.; McGillen, M. R.; Hamer, P. D.; Shallcross, D. E. *Physical Chemistry Chemical Physics* **2007**, *9*, 4338.

(10) Adachi, H.; Basco, N. *Chemical Physics Letters* **1979**, *64*, 431.

(11) Anastasi, C.; Waddington, D. J.; Woolley, A. *Journal of the Chemical Society-Faraday Transactions I* **1983**, *79*, 505.

(12) Andersson, B. Y.; Cox, R. A.; Jenkin, M. E. *International Journal of Chemical Kinetics* **1988**, *20*, 283.

(13) Christensen, L. E.; Okumura, M.; Sander, S. P.; Salawitch, R. J.; Toon, G. C.; Sen, B.; Blavier, J. F.; Jucks, K. W. *Geophysical Research Letters* **2002**, *29*.

(14) Anastasi, C. B., M.J.; Smith, D.B.; and Waddington, D.J. Joint Meeting of the French and Italian Sections of the Combustion Institute, June 1987, Amalfi.

(15) Atkinson, D. B.; Hudgens, J. W. *Journal of Physical Chemistry A* **1997**, *101*, 3901.

(16) Bauer, D.; Crowley, J. N.; Moortgat, G. K. *Journal of Photochemistry and Photobiology a-Chemistry* **1992**, *65*, 329.

(17) Fauvet, S.; Ganne, J. P.; Brion, J.; Daumont, D.; Malicet, J.; Chakir, A. *Journal De Chimie Physique Et De Physico-Chimie Biologique* **1997**, *94*, 484.

(18) Munk, J.; Pagsberg, P.; Ratajczak, E.; Sillesen, A. *Journal of Physical Chemistry* **1986**, *90*, 2752.

(19) Wallington, T. J.; Dagaut, P.; Kurylo, M. J. *Journal of Photochemistry and Photobiology a-Chemistry* **1988**, *42*, 173.

(20) Kaiser, E. W.; Rimai, L.; Wallington, T. J. *Journal of Physical Chemistry* **1989**, *93*, 4094.

(21) Niki, H.; Maker, P. D.; Savage, C. M.; Breitenbach, L. P. *Journal of Physical Chemistry* **1982**, *86*, 3825.

(22) Wallington, T. J.; Gierczak, C. A.; Ball, J. C.; Japar, S. M. *International Journal of Chemical Kinetics* **1989**, *21*, 1077.

(23) Lightfoot, P. D.; Cox, R. A.; Crowley, J. N.; Destriau, M.; Hayman, G. D.; Jenkin, M. E.; Moortgat, G. K.; Zabel, F. *Atmospheric Environment Part a-General Topics* **1992**, *26*, 1805.

(24) Christensen, L. E.; Okumura, M.; Sander, S. P.; Friedl, R. R.; Miller, C. E.; Sloan, J. J. *Journal of Physical Chemistry A* **2004**, *108*, 80.

(25) Kaiser, E. W. *Journal of Physical Chemistry* **1995**, *99*, 707.

(26) Clifford, E. P.; Farrell, J. T.; DeSain, J. D.; Taatjes, C. A. *Journal of Physical Chemistry A* **2000**, *104*, 11549.

(27) Kaiser, E. W.; Lorkovic, I. M.; Wallington, T. J. *Journal of Physical Chemistry* **1990**, *94*, 3352.

(28) DeSain, J. D.; Ho, A. D.; Taatjes, C. A. *Journal of Molecular Spectroscopy* **2003**, *219*, 163.

(29) Li, Y. M.; Sun, Q.; Li, H. Y.; Ge, M. F.; Wang, D. X. *Chinese Journal of Chemistry* **2005**, *23*, 993.

(30) Thiebaud, J.; Crunaire, S.; Fittschen, C. *Journal of Physical Chemistry A* **2007**, *111*, 6959.

(31) Sander, S. P.; Finlayson-Pitts, B. J.; Friedl, R. R.; Golden, D. M.; Huie, R. E.; Kolb, C. E.; Kurylo, M. J.; Molina, M. J.; Moortgat, G. K.; Orkin, V. L.; Ravishankara, A. R. "JPL 2006: Chemical Kinetics and Photochemical Data for Use in Atmospheric Studies, Evaluation No. 15, JPL Publication 06-2, Jet Propulsion Lab," 2006.

(32) Vaghjiani, G. L.; Ravishankara, A. R. *Journal of Chemical Physics* **1990**, *92*, 996.

(33) Christensen, L. E.; Okumura, M.; Hansen, J. C.; Sander, S. P.; Francisco, J. S. *Journal of Physical Chemistry A* **2006**, *110*, 6948.

(34) Taatjes, C. A.; Christensen, L. K.; Hurley, M. D.; Wallington, T. J. *Journal of Physical Chemistry A* **1999**, *103*, 9805.

(35) Wallington, T. J.; Skewes, L. M.; Siegl, W. O.; Wu, C. H.; Japar, S. M. *International Journal of Chemical Kinetics* **1988**, *20*, 867.

(36) Seakins, P. W.; Orlando, J. J.; Tyndall, G. S. *Physical Chemistry Chemical Physics* **2004**, *6*, 2224.

(37) Horie, O.; Crowley, J. N.; Moortgat, G. K. *Journal of Physical Chemistry* **1990**, *94*, 8198.

(38) Hasson, A. S.; Tyndall, G. S.; Orlando, J. J. *Journal of Physical Chemistry A* **2004**, *108*, 5979.

(39) Spittler, M.; Barnes, I.; Becker, K. H.; Wallington, T. J. *Chemical Physics Letters* **2000**, *321*, 57.

(40) Wallington, T. J.; Japar, S. M. *Chemical Physics Letters* **1990**, *166*, 495.

(41) Elrod, M. J.; Ranschaert, D. L.; Schneider, N. J. *International Journal of Chemical Kinetics* **2001**, *33*, 363.

(42) Hasson, A. S.; Kuwata, K. T.; Arroyo, M. C.; Petersen, E. B. *Journal of Photochemistry and Photobiology a-Chemistry* **2005**, *176*, 218.

(43) Hou, H.; Li, J.; Song, X. L.; Wang, B. S. *Journal of Physical Chemistry A* **2005**, *109*, 11206.

(44) Aloisio, S.; Francisco, J. S.; Friedl, R. R. *Journal of Physical Chemistry A* **2000**, *104*, 6597.

(45) Kanno, N.; Tonokura, K.; Tezaki, A.; Koshi, M. *Journal of Physical Chemistry A* **2005**, *109*, 3153.

(46) Kircher, C. C.; Sander, S. P. *Journal of Physical Chemistry* **1984**, *88*, 2082.

(47) Suma, K.; Sumiyoshi, Y.; Endo, Y. *Science* **2006**, *311*, 1278.

(48) English, A. M.; Hansen, J. C.; Szente, J. J.; Maricq, A. M. *Journal of Physical Chemistry A* **2008**, *112*, 9220.

(49) Dibble, T. S. *Atmospheric Environment Part a-General Topics* **2008**, *42*, 5837.

(50) Russell, G. A. *Journal of the American Chemical Society* **1957**, *79*, 3871.

(51) Ghigo, G.; Maranzana, A.; Tonachini, G. *Journal of Chemical Physics* **2003**, *118*, 10575.

(52) Feria, L.; Gonzalez, C.; Castro, M. *International Journal of Quantum Chemistry* **2004**, *96*, 380.